Cellular prion protein interaction with vitronectin supports axonal growth and is compensated by integrins

Glaucia N. M. Hajj[1,2], Marilene H. Lopes[1,3], Adriana F. Mercadante[4], Silvio S. Veiga[5], Rafael B. da Silveira[5], Tiago G. Santos[1,3], Karina C. B. Ribeiro[3], Maria A. Juliano[6], Saul G. Jacchieri[3], Silvio M. Zanata[4] and Vilma R. Martins[1,*]

[1]Ludwig Institute for Cancer Research, Hospital Alemão Oswaldo Cruz, São Paulo, Brazil
[2]Departamento de Bioquímica, Instituto de Química, Universidade de São Paulo, São Paulo, Brazil
[3]Centro de Tratamento e Pesquisa Hospital do Câncer, São Paulo, Brazil
[4]Departamento de Patologia Básica, Universidade Federal do Paraná, Curitiba, Brazil
[5]Departamento de Biologia Celular, Universidade Federal do Paraná, Curitiba, Brazil
[6]INFAR, Universidade Federal de São Paulo, São Paulo, Brazil
*Author for correspondence (e-mail: vmartins@ludwig.org.br)

Accepted 11 April 2007
Journal of Cell Science 120, 1915-1926 Published by The Company of Biologists 2007
doi:10.1242/jcs.03459

Summary

The physiological functions of the cellular prion protein, PrP^C, as a cell surface pleiotropic receptor are under debate. We report that PrP^C interacts with vitronectin but not with fibronectin or collagen. The binding sites mediating this PrP^C-vitronectin interaction were mapped to residues 105-119 of PrP^C and the residues 307-320 of vitronectin. The two proteins were co-localized in embryonic dorsal root ganglia from wild-type mice. Vitronectin addition to cultured dorsal root ganglia induced axonal growth, which could be mimicked by vitronectin peptide 307-320 and abrogated by anti-PrP^C antibodies. Full-length vitronectin, but not the vitronectin peptide 307-320, induced axonal growth of dorsal root neurons from two strains of PrP^C-null mice. Functional assays demonstrated that relative to wild-type cells, PrP^C-null dorsal root neurons were more responsive to the Arg-Gly-Asp peptide (an integrin-binding site), and exhibited greater $\alpha v\beta 3$ activity. Our findings indicate that PrP^C plays an important role in axonal growth, and this function may be rescued in PrP^C-knockout animals by integrin compensatory mechanisms.

Supplementary material available online at
http://jcs.biologists.org/cgi/content/full/120/11/1915/DC1

Key words: Dorsal root ganglia, Extracellular matrix, Cellular prion protein, Vitronectin, Axon growth, Integrins

Introduction

Cellular prion protein (PrP^C) is a cell-surface, glycosyl-phosphatidylinositol-anchored protein associated with several physiological functions. PrP^C is conserved among species and is expressed in most tissues, especially in the central nervous system and lymphoid tissues (Oesch et al., 1985). It has the ability to bind copper (Brown et al., 1997), to protect against oxidative stress (Brown and Besinger, 1998) and has been shown to influence cell signaling mechanisms, neuronal survival and differentiation (Chen, S. et al., 2003; Chiarini et al., 2002; Lopes et al., 2005; Mouillet-Richard et al., 2000). PrP^C has also been shown to bind the laminin receptor (Gauczynski et al., 2001; Hundt et al., 2001), to promote neuritogenesis through its interaction with NCAM (Santuccione et al., 2005; Schmitt-Ulms et al., 2001) and to induce neurite maintenance and neuronal differentiation through binding to the extracellular matrix (ECM) protein laminin (Ln) (Graner et al., 2000a; Graner et al., 2000b).

ECM proteins are known to regulate neuronal differentiation and axonal regeneration (Turney and Bridgman, 2005; Easley et al., 2006; Tom et al., 2004). Vitronectin (Vn) is expressed during development on embryonic day 10 (E10) in mice, mainly in the central nervous system (Seiffert et al., 1995), and has been shown to support proliferation and differentiation of cultured neurons (Martinez-Morales et al., 1995). In dorsal root ganglia (DRG) neurons, Vn-mediated axonal growth can be inhibited by anti-Vn antibody (Isahara and Yamamoto, 1995). Vn can also induce motor neuron differentiation, and anti-Vn antibodies reduce the number of motor neurons generated in chicken embryos (Martinez-Morales et al., 1997; Pons and Marti, 2000).

The classical ECM receptors, integrins, can bind several molecules and have been associated with ECM biological functions. The integrin recognition sequence Arg-Gly-Asp (RGD) is present in numerous ECM proteins including collagen, Vn and Fibronectin (Fn). RGD peptide is biologically active and able to substitute for ECM proteins in a variety of situations (Hynes, 2002; Pierschbacher and Ruoslahti, 1984).

Given that PrP^C binds Ln, we hypothesized that PrP^C might act as a broad ECM ligand and tested whether PrP^C binds the ECM proteins Vn, Fn and type IV collagen. We also sought to characterize the cellular events associated with any such binding. We assessed the role of PrP^C-ECM interaction in DRG

axon outgrowth using primary cultures obtained from two different PrP^C-null mouse strains (ZrchI and Npu) and their respective wild-type controls. The role of integrins in wild-type and PrP^C-null DRG axonal growth was also addressed and integrin activity was evaluated using specific antibodies and in functional assays using RGD peptide.

Results

PrP^C-vitronectin interaction

The first evidence of the PrP^C-Vn interaction was obtained with an overlay experiment (Fig. 1a), in which we applied equal mass aliquots of Vn, Ln, Fn, type IV collagen or bovine serum albumin (BSA) onto a nitrocellulose membrane, which was then incubated with ^{125}I-His_6-PrP^C. The overlay showed that PrP^C binds Ln, as previously demonstrated (Graner et al., 2000a), and also interacts with Vn (note that 10 μg of Ln represents 10 times fewer moles than the other proteins, owing to its higher molecular mass of ~900 kDa). Conversely, PrP^C did not associate with Fn or type IV collagen. Binding assays demonstrated that His_6-PrP^C binding to Vn is dose dependent and saturable (Fig. 1b), with a K_d of 12 nM. His_6-PrP^C refolded in the presence of copper (Zanata et al., 2002b) presented a similar binding to Vn (data not shown). It is important to note that the Vn used here was highly pure (see supplementary material Fig. S1a), and recombinant PrP^C analyzed by circular dichroism spectra showed an α-helix structure (Cordeiro et al., 2004a; Cordeiro et al., 2004b).

PrP^C interaction with ^{125}I-Vn could be blocked dose-dependently by competition with increasing concentrations of unlabeled Vn, as well as by other PrP^C ligands, such as stress-inducible protein 1 (STI1) (Zanata et al., 2002b) and Ln (Graner et al., 2000a; Graner et al., 2000b), but not by BSA (Fig. 1c). Thus, only specific PrP^C ligands can disrupt its binding interactions. The peptide representing the specific PrP^C binding site in the STI1 molecule (STI1 peptide) (Chiarini et al., 2002; Zanata et al., 2002b), but not that from Ln (Ln γ-1 peptide) (Graner et al., 2000a), competed for the PrP^C-Vn interaction (Fig. 1d). These data suggest that STI1 and Vn share a binding site in the PrP^C molecule, whereas Ln must interact with another PrP^C domain. Other Vn ligands such as type I collagen, type IV collagen and heparin were also tested for their ability to compete with the PrP^C-Vn interaction (supplementary material Fig. S2b). Although they do not bind Vn in the same domain as PrP^C (supplementary material Fig. S2a), they are able to disturb the PrP^C-Vn interaction, probably by steric hindrance.

Characterization of the PrP^C and Vn interacting domains

Of the twenty peptides from mouse PrP^C covering the whole protein sequence used to compete for PrP^C-Vn binding, two of them, corresponding to PrP^C residues 103-122 and 113-132,

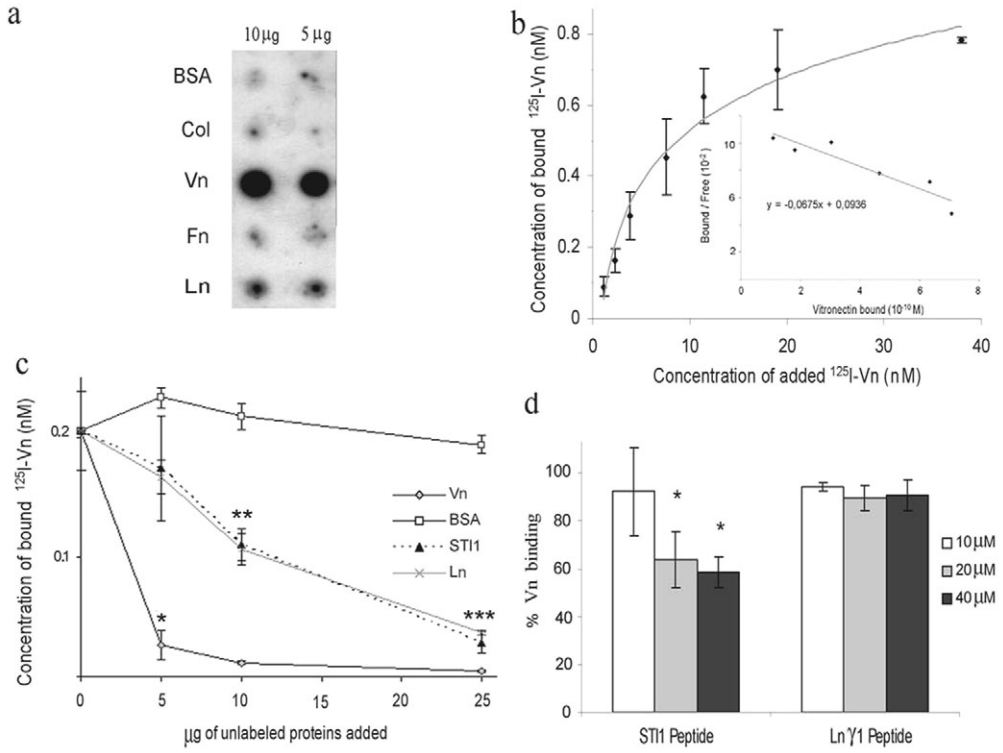

Fig. 1. Vn binds PrP^C in vitro and other PrP^C ligands can compete for this interaction. (a) Autoradiogram of overlay assay. Indicated amounts of Ln, Fn, Vn, type IV collagen (Col) and BSA were adsorbed onto a membrane and allowed to bind to ^{125}I-His_6-PrP^C. (b) PrP^C-coated wells were incubated with ^{125}I-Vn at the indicated concentrations. Wells were washed and radioactivity was measured. Scatchard plot is shown as an inset. The data represent mean ± s.d. (c) Competition assay in which ^{125}I-Vn was incubated over PrP^C-coated wells in the presence of increasing concentrations of unlabeled Vn, STI1, Ln or BSA. Bound ^{125}I-Vn differed from addition of 5 μg unlabeled Vn (*P<0.001), addition of 10 μg unlabeled Vn or Ln (**P<0.001), or addition of 25 μg unlabeled Vn, Ln or STI1 (***P<0.001) according to Tukey's Test. (d) Competition assay in which ^{125}I-Vn was incubated over PrP^C-coated wells in the presence of increasing concentrations of unlabeled STI1 peptide or Ln γ-1 peptide. The percentage of Vn binding was reduced in the presence of 20 or 40 μM STI1 peptide (*P<0.02, Student's t-test).

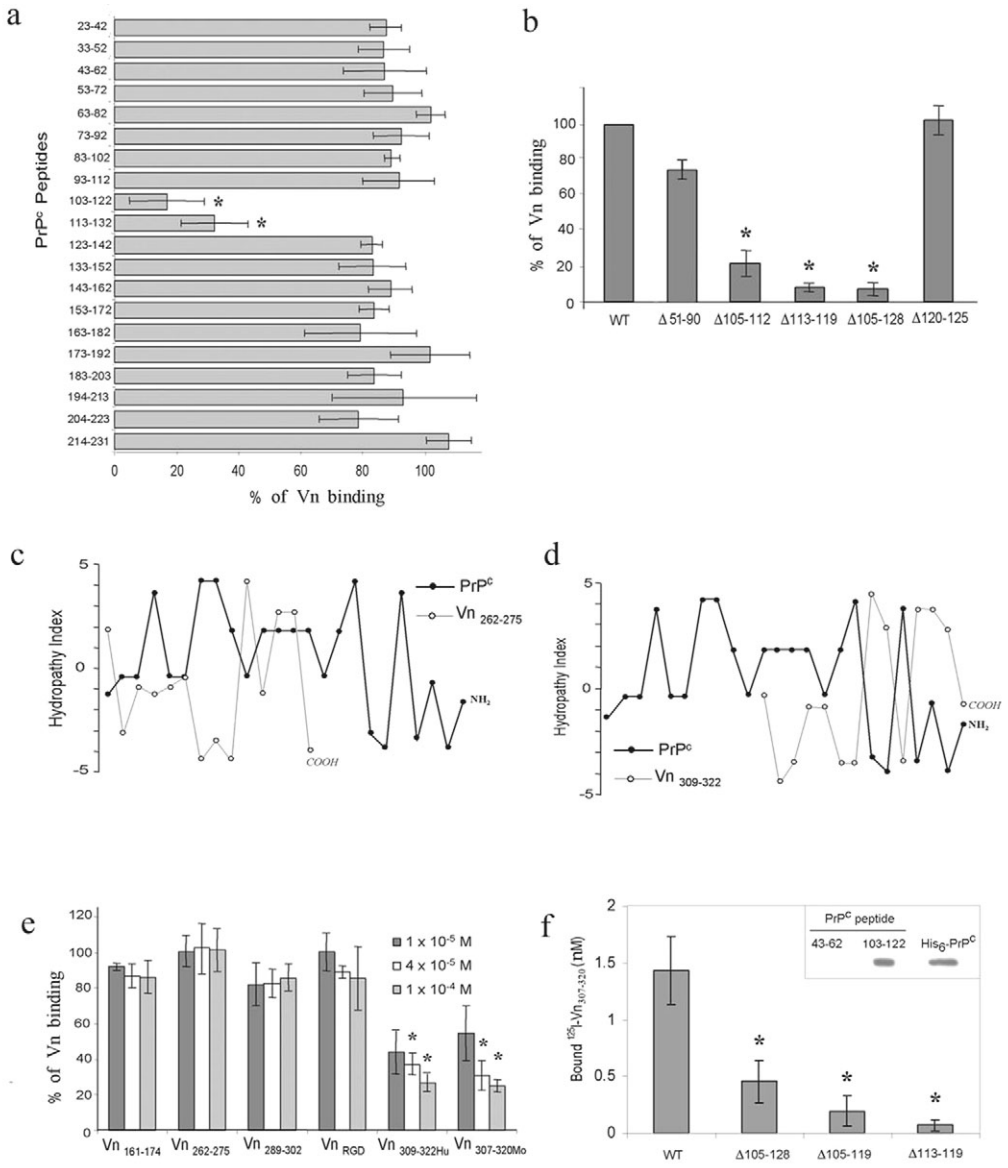

Fig. 2. Mapping the binding sites within Vn and PrP^C. (a) ^{125}I-Vn was incubated over PrP^C coated wells in the presence of PrP^C peptides. Binding to PrP^C was set as 100% and binding in the presence of peptides was expressed as a percentage thereof. PrP^C peptides 103-122 and 113-132 interfered with binding to Vn (*P<0.01, Student's t-test). (b) ^{125}I-Vn binding to deletion mutant proteins Δ105-112, Δ113-119, or Δ105-128 His$_6$-PrP^C was markedly reduced relative to binding to wild-type PrP^C, which was set as 100% (*P<0.01, Student's t-test). Δ51-90 and Δ120-125 His$_6$-PrP^C proteins exhibited ^{125}I-Vn binding that did not differ significantly from the wild-type protein. (c,d) The hydropathy plots compare the mouse PrP^C amino acid sequence from a.a. 104 to 127 and human Vn peptides with complementary hydropathy pattern: (c) Vn$_{262-275}$ and (d) Vn$_{309-322}$. (e) ^{125}I-Vn was incubated in PrP^C-coated wells in the presence or absence of the indicated concentrations of Vn peptides and radioactivity levels were determined. ^{125}I-Vn binding was disrupted in the presence of Vn$_{309-322Hu}$ and Vn$_{307-320Mo}$ (*P<0.01 vs binding to PrP^C alone, Student's t-test) at the two higher concentrations tested. (f) Binding of peptide Vn$_{307-320Mo}$ to immobilized PrP^C. Wells were coated with wild-type, Δ105-119, Δ113-119 or Δ105-128 His$_6$-PrP^C proteins and incubated with 1 μM ^{125}I-Vn$_{307-320Mo}$. ^{125}I-Vn$_{307-320Mo}$ binding to immobilized PrP^C was reduced in Δ105-128, Δ105-119 or Δ113-119 His$_6$-PrP^C proteins relative to wild-type PrP^C controls (*P<0.001, Tukey's test). Inset shows an overlay assay, where His$_6$-PrP^C or PrP^c peptides 43-62 and 103-122 spotted into a membrane were incubated with biotin labeled Vn$_{307-320Mo}$ followed by streptavidin-HRP.

effectively blocked (by ~80%) PrP^C-Vn binding (Fig. 2a). This implies that the amino acid sequence shared by both peptides may represent the putative binding site for Vn in the PrP^C molecule. The binding and competition assays were always performed with a freshly prepared peptide solution to avoid possible neurotoxic aggregates (Chiarini et al., 2002; Ettaiche et al., 2000). The lack of PrP^C-Vn interaction blockade by peptide 93-112, which can also form aggregates owing to the partial presence of the hydrophobic domain, provides further evidence that the interaction blockade was not the result of peptide aggregation.

Binding assays performed using four PrP^C molecules presenting small deletions on the putative Vn binding site, revealed that the PrP^C deletion mutants Δ105-112, Δ113-119,

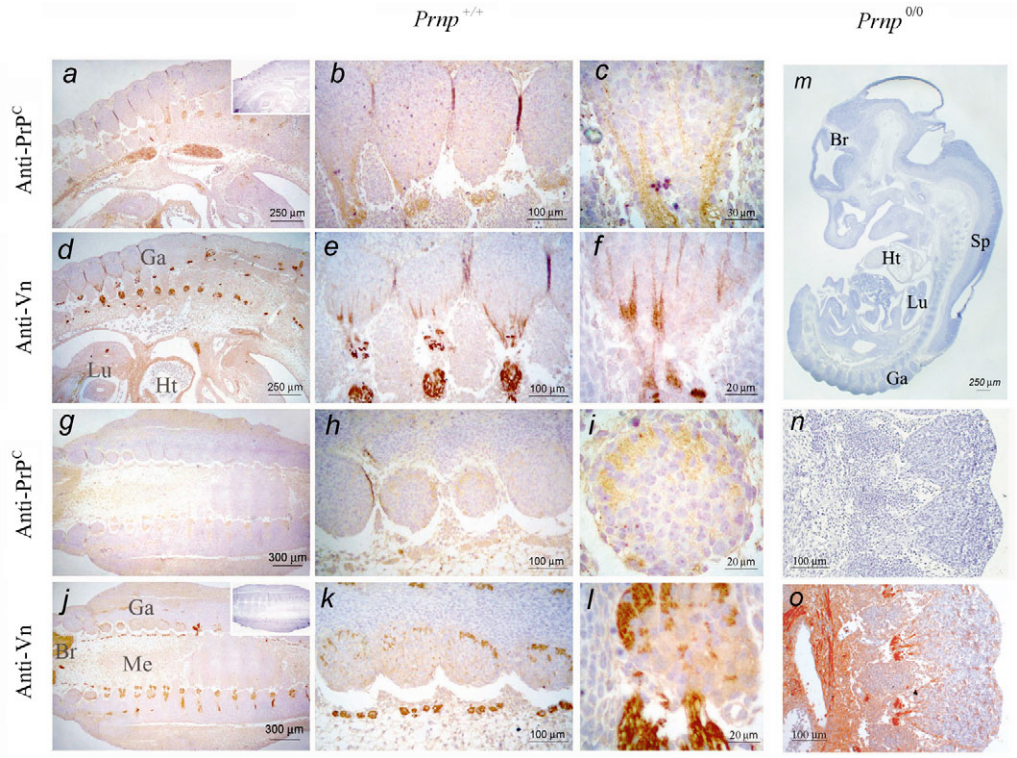

Fig. 3. PrP^{C} and Vn expression in mouse embryos. E12.5 *Prnp*$^{+/+}$ sagittal (a-f) or coronal (g-l) sections reacted with anti-PrP^{C} mouse serum (a,b,c,g,h,i), rabbit serum anti-Vn (d,e,f,j,k,l) or non-immune mouse or rabbit serum (insets in panels a and j, respectively). E12.5 ZrchI *Prnp*$^{0/0}$ mouse sagittal sections reacted with anti-PrP^{C} mouse serum (m and n) or anti-Vn serum (panel o). Br, brain; Ht, heart; Lu, lung; Sp, spinal cord; Ga, dorsal root ganglia.

and Δ105-128 did not bind Vn, whereas mutants Δ51-90 and Δ120-125 exhibited binding capacity similar to that of the wild-type molecule (Fig. 2b). These data corroborate that the region comprising a.a. 105-119 of PrP^{C} includes the binding site for Vn. As this domain is inserted into the N-terminal random coil of the PrP^{C} molecule (Riek et al., 1996), these deletions are not expected to disturb PrP^{C} secondary or tertiary structure. Since all the experiments herein were conducted with *E. coli* recombinant His$_{6}$-PrP^{C}, we were unable to evaluate possible roles of PrP^{C} sugar residues in this interaction. However, as the binding site was mapped to a region lying outside the glycosylation site, it is unlikely that sugar residues on PrP^{C} are essential for its interaction with Vn.

In accordance with the complementary hydropathy theory (Brentani, 1988), which states that peptides presenting opposite hydropathy profiles can bind one another, we used HYDROLOG software to search for Vn sequences whose hydropathy profile was more than 70% complementary to the PrP^{C} 105-119 peptide. Two human Vn domains presented this profile, one from residues 262-275 (Fig. 2c) and another from residues 309-322 (Fig. 2d). We performed competition assays using both peptides and, as controls, two peptides randomly chosen from within the Vn sequence (Vn$_{161\text{-}174}$ and Vn$_{289\text{-}302}$) along with a peptide containing the RGD sequence (Vn$_{RGD}$) (Ruoslahti and Pierschbacher, 1987). The peptides Vn$_{309\text{-}322Hu}$ (human Vn) and Vn$_{307\text{-}320Mo}$ (the equivalent peptide for mouse Vn) competed for PrP^{C}-Vn interaction, thus identifying this domain as the putative binding site for PrP^{C} (Fig. 2e).

We also performed binding assays using the ^{125}I-Vn$_{307\text{-}320Mo}$ peptide and wild-type His$_{6}$-PrP^{C} or PrP^{C} deletion mutants Δ105-128, Δ105-119 and Δ113-119. Vn$_{307\text{-}320Mo}$ peptide readily bound wild-type PrP^{C}, whereas very low binding was observed with all of the deletion mutants (Fig. 2f). Using overlay assays we demonstrated that peptide Vn$_{307\text{-}320Mo}$ directly binds the PrP^{C} peptide corresponding to a.a. 103-122, but not to a.a. 43-62 (Fig. 2f inset). These data are consistent with the presence of an interaction between the PrP^{C} domain 105-119 and the Vn domain 307-320 (mouse Vn).

Supplementary material Fig. S2a shows a schematic representation of PrP^{C} and Vn, along with their main ligands and respective binding sites (Lee et al., 2003; Schvartz et al., 1999). Although there is moderate sequence diversity in Vn across species, the PrP^{C} binding domain is generally well-conserved (see supplementary material Fig. S3a). Chicken Vn, which has the greatest divergence relative to human Vn, bound PrP^{C} in the same manner as human Vn (see supplementary material Fig. S3b). Furthermore, peptides from the PrP^{C}-binding domain derived from chicken and mouse Vn sequences were also able to inhibit the PrP^{C} interaction with human Vn (see supplementary material Fig. S3c), suggesting that the PrP^{C}-Vn interaction is evolutionarily conserved.

PrP^{C} and Vn expression in DRG from embryonic mice

Since Vn and PrP^{C} have been detected early in development (Miele et al., 2003; Seiffert et al., 1995), we performed immunohistochemistry assays in E12.5 mice embryos.

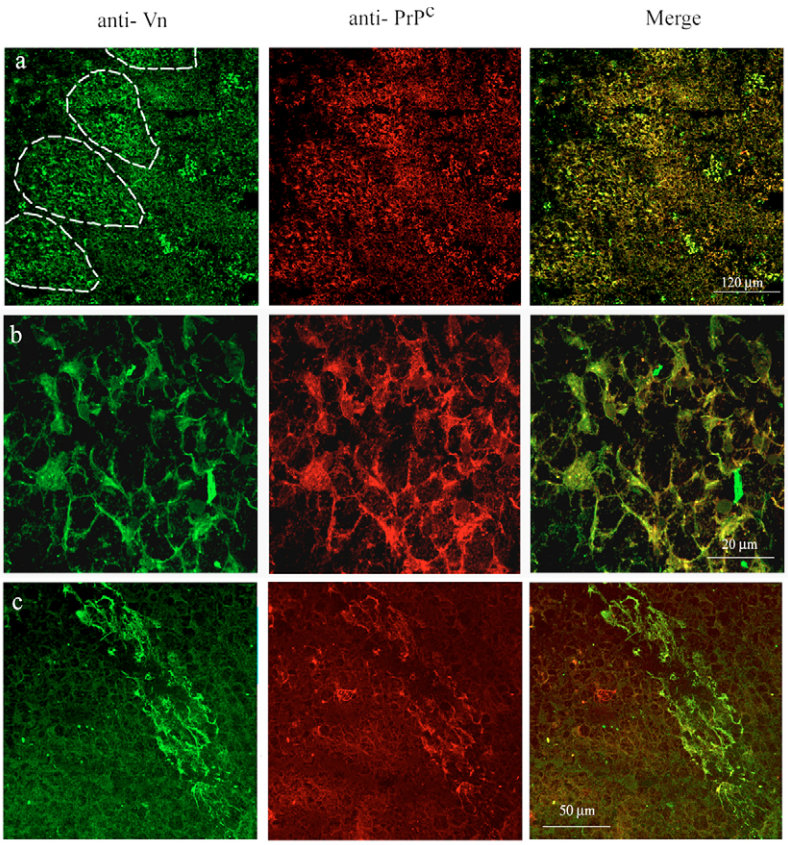

Fig. 4. PrP^C and Vn colocalize in embryonic DRG. Confocal microscopy images of E12.5 mouse sagittal sections reacted with anti-Vn rabbit serum (green) and anti-PrP^C mouse serum (red). Superimposed red and green images are shown in the merge column. The top row of images (a) shows three ganglia in a low magnification (as indicated by the dotted lines); the middle row of images (b) shows a single ganglion in a higher magnification; and the bottom row (c) shows a growing nerve region.

Immunohistochemistry assays were performed in ZrchI *Prnp*$^{+/+}$ (Fig. 3a-l) and ZrchI *Prnp*$^{0/0}$ (Fig. 3m-o) E12.5 mice embryos using anti-PrP^C (Fig. 3a-c,g-i,m,n) and anti-Vn antibodies (Fig. 3d-f,j-l,o) in sagittal sections (Fig. 3a-f,m-o) and coronal sections (Fig. 3g-l). The antibodies used have been extensively tested in western blotting assays, and show specificity for PrP^C (Zanata et al., 2002b) or Vn (data not shown). Control experiments with mouse or rabbit serum produced no immunolabeling (Fig. 3 insets in a and j, respectively).

In accordance with previous data (Miele et al., 2003), we observed strong PrP^C immunoreactivity in the developing brain, spinal cord (Fig. 3g) and DRG (Fig. 3a,g). In DRG, although axons and forming axonal fibers were heavily labeled, nuclei were not labeled and neuronal bodies showed only weak labeling (Fig. 3b,c,h,i). PrP^C expression could be detected only at E10, in the nervous system and in the heart (data not shown). As development proceeds, those organs still show high levels of immunoreactivity. Immunolabeling in other organs such as kidney, lungs and muscles could only be seen later (E18) in development (data not shown). Sections from Prnp$^{0/0}$ mouse embryos did not bind the anti-PrP^C antibody, proving the specificity of the immunohistochemistry reaction (Fig. 3m,n).

Vn immunolabeling was more intense than PrP^C, but presented a similar pattern in brain, spinal cord (Fig. 3j) and DRG (Fig. 3d,j). In the DRGs, expression was predominantly observed in growing axons and nerves (Fig. 3e,f,k,l). Vn starts to be expressed at E8, through the whole embryo. Similarly to PrP^C, at E10 it presents high expression in the heart and nervous system. As development proceeds, those organs still present high levels of immunoreactivity, whereas immunolabeling can also be seen in other organs such as kidney, lung and muscles. Expression in the liver is very abundant (data not shown), since this organ secretes Vn to the blood. In PrP^C-null mice, the pattern of Vn expression in DRG (Fig. 3o) as well as in other tissues (data not shown) was the same as that in wild-type mice. Immunofluorescent confocal images confirmed that PrP^C and Vn strongly co-localized in DRG cells (Fig. 4a,b) and in growing nerves (Fig. 4c).

Vn binds PrP^C in vivo

To verify whether Vn could bind PrP^C in the cell surface, we labeled Vn with Alexa Fluor 568 (see supplementary material Fig. S1b). Dissociated DRG cells were treated with Alexa 568-Vn and subjected to PrP^C fluorescent immunocytochemistry (Fig. 5a upper panel). We observed the co-localization of Vn and PrP^C at the cell surface. Images of live SN-56 cells (Blusztajn et al., 1992; Hammond et al., 1990) transfected with green fluorescent protein (GFP)-PrP^C and treated with Alexa 568-Vn showed co-localization of PrP^C with Vn at the cell surface (Fig. 5a bottom panel).

SDS-PAGE of GFP-PrP^C-transfected HEK293 cell proteins eluted from a pull-down assay using purified Vn covalently coupled to CNBr-Sepharose followed by immunoblotting, revealed a band of ~60 kDa [the expected molecular mass for GFP-PrP^C (Lee et al., 2001)] when anti-GFP (lane 3) or anti-PrP^C antibodies (lane 6) were applied (Fig. 5b). When the same procedure was conducted with extracts from non-transfected cells (lanes 1 and 4) or with those from cells transfected with GFP alone (lanes 2 and 5) no binding to the Vn-Sepharose was observed. These results indicate that PrP^C, but not GFP alone, binds to Vn. The levels of endogenous PrP^C in HEK293 cells were too low for their association with Vn to be detected.

PrP^C-Vn interaction mediates DRG axonal growth

We investigated the possible role in axonal growth of the interaction between PrP^C and Vn, which are expressed in elongating DRG and medulla axons and are implicated in neuronal differentiation (Graner et al., 2000a; Graner et al., 2000b; Martinez-Morales et al., 1995; Martinez-Morales et al., 1997; Pons et al., 2001; Sales et al., 2002). Cultured DRG explants from E12.5 mice expressing PrP^C (ZrchI *Prnp*$^{+/+}$) (Fig. 6a inset) in the presence of Vn for 36 hours produced axonal growth (Fig. 6a). Vn peptide, Vn$_{307\text{-}320\text{Mo}}$, corresponding to the PrP^C-binding site of the mouse Vn molecule elicited the same effect as that triggered by the whole molecule (Fig. 6b), whereas Vn peptide Vn$_{161\text{-}174}$ (Fig. 6d) had

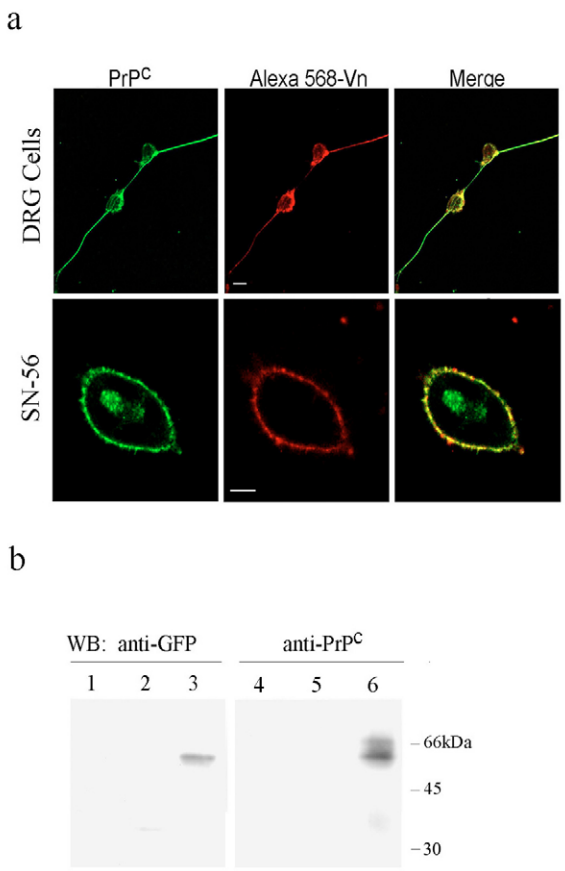

Fig. 5. Vn binds PrP^C in vivo. (a) Confocal images of dissociated DRG cells treated with Alexa 568-Vn (red) and immunolabeled with anti-PrP^C (green) are shown in the top row. Confocal images of SN56 cells transfected with GFP-PrP^C (green) and treated with Alexa 568-Vn (red) are shown in the bottom row. (b) Pull down assay from cell extracts incubated with Vn-Sepharose. Western blots of Vn-Sepharose-bound proteins from untransfected (lanes 1 and 4), GFP transfected (lanes 2 and 5) or GFP-PrP^C transfected (lanes 3 and 6) HEK293 cells. Blots immunolabeled with anti-GFP (lanes 1 to 3) or anti-PrP^C (lanes 4 to 6) antibodies revealed that PrP^C, but not GFP alone, binds to Vn.

no effect, even at concentrations 20-fold higher than peptide $Vn_{307\text{-}320Mo}$.

ZrchI *Prnp*$^{0/0}$ mouse (Bueler et al., 1992) DRG neurons cultured on Vn presented neurite growth rates (Fig. 6g) similar to that of wild-type DRG neurons (Fig. 6a). Nevertheless, in opposition to what has been demonstrated for wild-type DRG, Vn peptide $Vn_{307\text{-}320Mo}$ (Fig. 6f), which mimics the PrP^C binding site, was unable to induce axon growth in *Prnp*$^{0/0}$ DRG neurons. Vn peptide $Vn_{161\text{-}174}$ also had no effect on *Prnp*$^{0/0}$ DRG neurons (Fig. 6e). Treatment of Vn-stimulated DRG with rabbit anti-PrP^C antibody blocked axonal growth in cultures from wild-type animals but not in those from PrP^C-null mice (Fig. 6h). Data representing the average axon length from each treatment are summarized in Fig. 6h.

To rule out the possibility of spurious results because of genetic background, we conducted our key experiments in both ZrchI (Bueler et al., 1992) and Npu (Manson et al., 1994) PrP^C-null mice. DRG from Npu *Prnp*$^{-/-}$ mice and their wild-type controls plated for 24 hours in the presence of Vn presented similar axonal growth (Fig. 6i). On the other hand, when plated with $Vn_{307\text{-}320Mo}$, only Npu *Prnp*$^{+/+}$ DRG grew axons and no effect was observed with either knockout or wild-type cells when an irrelevant Vn peptide ($Vn_{161\text{-}174}$) was used (Fig. 6i). Inclusion of an antibody against PrP^C peptide 106-126 (Chiarini et al., 2002) (Fig. 6i) completely blocked axonal growth in cultures from wild-type animals, whereas non-immune purified IgG had no effect (Fig. 6i). We also carried out dissociated DRG cell cultures in the presence of Vn to measure the percentage of cells with neurites, and observed that the positive responsiveness to Vn was the same for ZrchI *Prnp*$^{+/+}$ and *Prnp*$^{0/0}$ neurons (Fig. 6j).

The experiments using anti-PrP^C antibodies or the $Vn_{307\text{-}320}$ peptide demonstrated that axonal growth can be supported specifically by the PrP^C-Vn interaction. Nonetheless, the whole Vn molecule induces the same axonal outgrowth pattern in wild-type and PrP^C-null neurons. The similarity between the effect of Vn in wild-type and PrP^C-null DRG suggests that there may be another Vn receptor that can compensate for the PrP^C deficiency.

In fact, flow cytometry analysis shows that Alexa 568-Vn is able to bind equally to the surface of PrP^C-null and wild-type cells (see supplementary material Fig. S4a). Indicating that in the absence of PrP^C other Vn receptors are present at the cell surface.

Integrin participation in Vn-induced axonal growth is enhanced in the absence of PrP^C

The obvious targets for the putative compensatory mechanism suggested by the above data are integrins, the classical Vn receptors that interact with this molecule through the Vn-RGD peptide. We performed functional assays using the RGD peptide, which has an advantage over antibodies in that it can simultaneously trigger or halt several integrin dimers (Isahara and Yamamoto, 1995; Monier-Gavelle and Duband, 1997). The RGD peptide can be used for inhibition or stimulation of the neuritogenesis depending on its presentation. In solution, the RGD peptide does not support cell adhesion and thus can be used to perform competition assays (Pierschbacher and Ruoslahti, 1987). Conversely, when coupled to BSA, the peptide adheres to the coverslip and supports cell adhesion (Danilov and Juliano, 1989).

As shown in Fig. 7a, the Vn_{RGD} peptide at a concentration of 8 μM inhibited Vn-stimulated axonal growth of ZrchI *Prnp*$^{0/0}$ DRG neurons. The impairment reached poly-L-lysine growth levels (about 50% of that observed in Vn). Vn-stimulated axonal growth in *Prnp*$^{+/+}$ neurons was impaired only when the Vn_{RGD} peptide reached a concentration of 12 μM. Additionally, we measured the axonal growth induced by Vn_{RGD}-BSA and observed that ZrchI *Prnp*$^{0/0}$ DRG are more responsive than *Prnp*$^{+/+}$ DRG (Fig. 7b). *Prnp*$^{0/0}$ DRG neurons extended axons in 0.5 nmol of adsorbed peptide, whereas *Prnp*$^{+/+}$ DRG neurons did not exhibit any axonal growth, even in the presence of a 20-fold higher concentration of the peptide. Thus, *Prnp*$^{0/0}$ DRG cells were more responsive than the *Prnp*$^{+/+}$ cells to the RGD peptide. To further confirm these results, we plated Npu *Prnp*$^{-/-}$ and *Prnp*$^{+/+}$ DRG over adsorbed RGD-BSA. We observed that Npu *Prnp*$^{-/-}$ DRG neurons were also more responsive to RGD-BSA than Npu *Prnp*$^{+/+}$ DRG neurons (Fig. 7c). Thus, we can be confident that the above

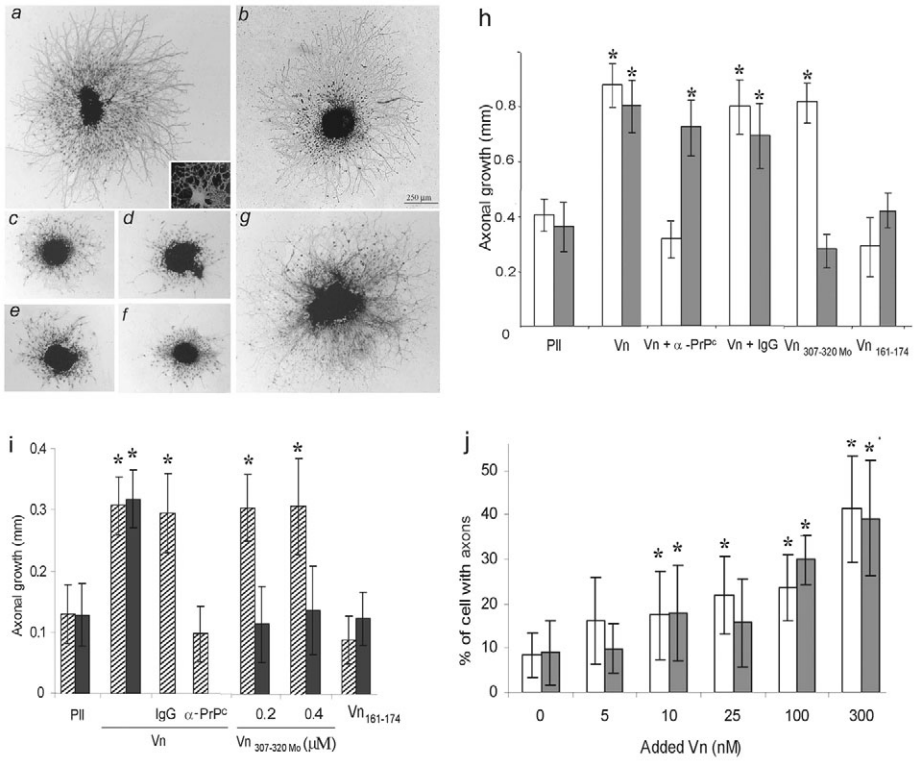

Fig. 6. PrP^{C}-Vn interaction supports axonal growth in DRG from E12.5 mouse embryos. ZrchI *Prnp*$^{+/+}$ (a-d) and ZrchI *Prnp*$^{0/0}$ (e-g) DRG were cultured on poly-L-lysine-coated coverslips (c), 200 nM Vn (a and g), 0.4 μM peptide Vn$_{307-320Mo}$ (b and f), 0.4 μM peptide Vn$_{161-174}$ (d and e) and Vn plus anti-recombinant PrP^{C} antibody 13 μg/ml or Vn plus irrelevant IgG 13 μg/ml (h). Inset dark-field image in a shows a DRG subjected to anti-PrP^{C} immunohistochemistry. (h) Comparison of mean axonal growth per DRG from ZrchI *Prnp*$^{+/+}$ (white bars) and *Prnp*$^{0/0}$ mice (grey bars) for the conditions described above. *P<0.001 vs Pll control, Tukey's Test. (i) Comparison of mean axonal growth per DRG of at least 12 ganglia from Npu *Prnp*$^{+/+}$ (striped bars) and *Prnp*$^{-/-}$ mice (black bars) for each of the following conditions: Pll, 200 nM Vn, 0.2 or 0.4 μM Vn$_{307-320Mo}$, 0.4 μM Vn$_{161-174}$, Vn plus irrelevant IgG or 0.6 μg/ml anti-PrP^{C} peptide 106-126. *P<0.001 vs Pll control, Tukey's Test. (j) The percentage of cells from ZrchI *Prnp*$^{+/+}$ (white bars) and ZrchI *Prnp*$^{0/0}$ (grey bars) dissociated DRG neurons that grow axons increased with increasing concentrations of Vn; *P<0.001 vs Pll control, Tukey's test.

findings were not due to any spurious effect present only in ZrchI animals. These data demonstrate that PrP^{C}-ablated DRG neurons have a greater dependence upon integrins for axonal outgrowth than do their respective wild-type cells.

To test whether the activation state of Vn-binding integrins was altered, we measured the level of active αvβ3 integrin in adhering ZrchI *Prnp*$^{0/0}$ DRG cells through an immunofluorescence assay with the ligand-mimetic antibody WOW-1 (Pampori et al., 1999). ZrchI *Prnp*$^{0/0}$ DRG neurons showed a 30% higher level of αvβ3 activation than *Prnp*$^{+/+}$ DRG neurons (Fig. 7d). We tested whether Npu *Prnp*$^{-/-}$ neurons presented a similar increase in integrin activity using the commercially available anti-ligand-induced binding sites (LIBS) antibody AP5 (Faccio et al., 2002). Dissociated Npu *Prnp*$^{-/-}$ DRG neurons showed greater β_3 activity than *Prnp*$^{+/+}$ cells (Fig. 7e). Accordingly, ZrchI *Prnp*$^{0/0}$ primary mouse embryonic fibroblasts (PMEFs) also showed 30% more integrin αv subunit expression than wild-type PMEFs (see supplementary material Fig. S4b). Together, these findings indicate that a higher integrin activity, particularly that from αvβ3 integrin, is present in DRG after ablation of PrP^{C}.

Discussion

In the past few years, many PrP^{C}-binding proteins have been identified. Among these the ECM protein Ln (Graner et al., 2000a; Graner et al., 2000b) and glycosaminoglycans (Gonzalez-Iglesias et al., 2002) have been of particular interest. These previous findings suggested that PrP^{C} might act as a wide-range cell surface receptor, capable of binding numerous ECM proteins. However, the present findings indicate that PrP^{C} interaction with ECM proteins is not a broad-spectrum phenomenon, but rather that PrP^{C} specifically binds Vn with high affinity, and does not readily bind Fn or type IV collagen.

We proposed that PrP^{C} participates in a multi-protein complex, the biological effects of which would be dependent both on the affinity and accessibility of each member of the complex (Martins and Brentani, 2002). The present competition experiments demonstrated that PrP^{C}-Vn interaction in vitro has a higher affinity, K_d 10^{-8} M, than that between PrP^{C} and STI1, K_d 10^{-7} M (Zanata et al., 2002b). Furthermore, the Vn binding domain in PrP^{C} in residues 105-119 (Fig. 2a) overlaps with the STI1-binding domain (Zanata et al., 2002b), indicating that PrP^{C} interactions with Vn or STI1 are mutually exclusive, with the first being more favorable and conditioning the latter to local protein availability and levels. The ability of PrP^{C}-STI1 to provide neuroprotection against programmed cell death (Chiarini et al., 2002) and neuritogenesis in hippocampal neurons (Lopes et al., 2005), whereas PrP^{C}-Vn engagement promotes axonal growth in DRG, provide prime examples of how cell fate can be directly influenced by the molecular environment of the cell.

PrP^{C} domain 105-128, which contains the Vn and STI1 binding sites, is highly conserved across species (Gabriel et al., 1992), and is indeed identical in mice and humans. This domain also includes proteolytic sites (Jimenez-Huete et al., 1998) and hereditary prion disease-associated mutations (Mastrianni and Roos, 2000), indicating that this region and probably its interaction with Vn and STI1 have an important role in vivo. For example, it was recently reported that this domain is linked to the toxicity of PrP^{C} accumulated in the cytosol through binding to Bcl-2 (Rambold et al., 2006).

Although PrP^{C}-Ln and PrP^{C}-Vn interactions present a similar K_d, (Graner et al., 2000a), we demonstrated that lower concentrations of Vn than Ln are needed to disrupt the PrP^{C}-Vn interaction. Since the Ln-binding site is located in residues 173-183 of PrP^{C} (Coitinho et al., 2006), the Ln γ1 peptide (the

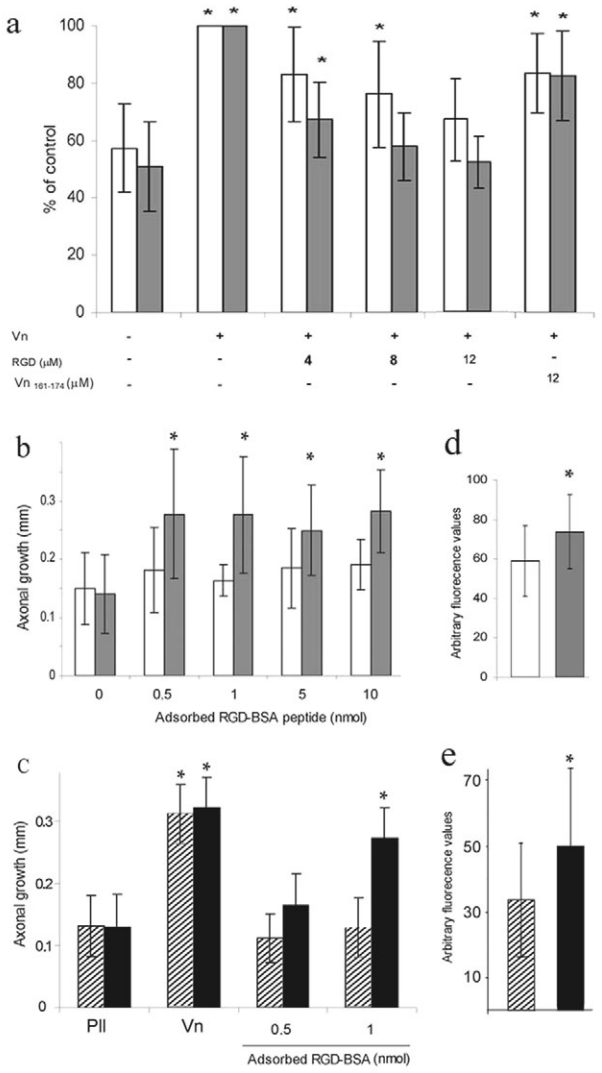

Fig. 7. Integrins compensate for the absence of PrP^C to support Vn-induced axonal growth. (a) Vn_{RGD} peptide abrogates Vn-induced axonal growth in cultured ZrchI *Prnp*$^{0/0}$ (grey bars) DRGs at lower concentrations (8 μM) than that (12 μM) necessary for the same effect in *Prnp*$^{+/+}$ (white bars) DRGs. Treatment with the irrelevant peptide $Vn_{161\text{-}174}$ (12 μM) had no effect. **P*<0.001 vs poly-L-lysine (Pll) Tukey's test. (b) Exposure to adsorbed Vn_{RGD}-BSA peptide (0.5, 5, 1 or 10 nmol) increased axonal growth in DRG cells from ZrchI *Prnp*$^{0/0}$ mice, but not from ZrchI *Prnp*$^{+/+}$ mice. **P*<0.001 vs Pll control, Tukey's test. (c) Adsorbed Vn_{RGD}-BSA peptide (1 nmol) induced axonal growth in cultured DRG cells from Npu *Prnp*$^{-/-}$ mice (black bars) whereas no axonal growth was present at this concentration of absorbed Vn_{RGD}-BSA peptide in Npu *Prnp*$^{+/+}$ cells (striped bars). **P*<0.001 vs Pll control, Tukey's test. (d) ZrchI *Prnp*$^{0/0}$ dissociated DRG cells exhibited greater WOW-1 immunoreactivity than those from ZrchI *Prnp*$^{+/+}$ mice, indicating that the knockouts had greater levels of activated $\alpha_v\beta_3$ integrin. **P*<0.001 vs *Prnp*$^{+/+}$, Mann-Whitney's test. (e) Npu *Prnp*$^{-/-}$ dissociated DRG cells exhibited greater AP5 immunoreactivity than Npu *Prnp*$^{+/+}$, indicating that the knockouts had greater levels of activated β_3 integrin. **P*<0.001 vs Npu *Prnp*$^{+/+}$, Mann-Whitney's test.

PrP^C-binding site in Ln) does not disrupt the PrP^C-Vn complex (Fig. 1d). Thus, it is plausible that in vitro, the Ln molecule may interact with PrP^C, and thereby disturb PrP^C-Vn binding by steric hindrance. On the other hand, steric hindrance may not occur in vivo because of the ECM organization or to the presence of biologically active proteolytic fragments from the Ln molecule (Chen, Z. et al., 2003). Indeed, the signals triggered by each of these PrP^C ligands may have cooperative roles in some biological events. In developing cerebellar granule cells, the presence of Ln induces proliferation, whereas during migration these cells find Vn and differentiate (Pons et al., 2001). Therefore, we believe that PrP^C has pleiotropic functions that depend upon its cellular expression as well as the greater contextual cellular milieu.

We exploited the complementary hydropathy principle (Brentani, 1988) to map a.a. 309-322 as the PrP^C-binding site in the human Vn molecule. To date, more than 40 protein-protein interactions have been shown to comply with this principle (Heal et al., 2002), including a Vn and fibrinogen interaction with the integrin αIIbβ3 (Gartner et al., 1991) and the PrP^C-STI1 interaction (Martins et al., 1997; Zanata et al., 2002b). This region (residues 309-322) of human Vn has never been shown to bind other proteins (Schvartz et al., 1999). According to the three-dimensional theoretical model of Vn (Xu et al., 2001), this mainly hydrophobic peptide is partially buried. Conversely, it should be considered that the threading algorithm (Xu and Xu, 2000) used to create this model makes use of an energy function that penalizes the exposure of hydrophobic side chains, whereas it is known that protein-binding sites are generally hydrophobic (Tsai et al., 1997). Since it was not considered that this particular region could be a binding site, protein interactions were not taken into consideration in these calculations (Xu et al., 2001).

Vn is composed of multiple domains known to bind distinct proteins (see supplementary material Fig. S2a). The first 44 amino acids comprise a somatomedin-like domain, which harbors plasminogen activator inhibitor-1. This somatomedin-like domain is followed by the RGD peptide domain (residues 53-64), which is responsible for integrin binding, and an acidic stretch involved in binding of the thrombin-antithrombin III complex. Two binding sites for collagen have been described, one adjacent to the RGD site and other adjacent to the heparin-binding site. The Vn is composed of six hemopexin domains (a.a. 132-459). The C-terminal part of the molecule harbors a plasminogen (a.a. 332-348), a heparin (a.a. 348-346) and a glycosaminoglycan-binding site (a.a. 348-361). A subregion of this domain (a.a. 348-370) has also been implicated in plasminogen activator inhibitor-1 binding (Preissner, 1991; Schvartz et al., 1999). Thus although the PrP^C-binding site in Vn has not been assigned to bind other proteins, it is close to the heparin-binding domain. Heparin is efficient in competing PrP^C-Vn interaction (see supplementary material Fig. S2a), since it is able to bind both PrP^C (Pan et al., 2002) and Vn (Francois et al., 1999). Thus, as proposed above, PrP^C pleiotropic functions are dependent on the greater contextual cellular milieu.

There are many Vn receptors found on the cell surface, such as integrins αIIbβ3, αvβ1, αvβ3 and αvβ5 (Felding-Habermann and Cheresh, 1993). Each one of these binds to the Vn RGD domain with a different affinity and induces specific signals within cells (Takagi et al., 2002). Our demonstration herein that RGD peptide did not compete for the PrP^C-Vn

interaction indicates that Vn binds PrP^C at a domain that is distinct from the integrin-binding domain.

Since both PrP^C and integrins participate in axonal growth, it was surprising to observe a complete inhibition of Vn-stimulated axonal growth in the presence of anti-PrP^C antibody. This finding suggests that PrP^C occupies a part of the macromolecular complex such that its inactivation by antibodies may disturb the whole complex. The ability of Vn peptide containing the PrP^C-binding site to reproduce the biological effects of the whole Vn in wild-type but not in PrP^C-null DRG, further suggests that PrP^C is an exclusive ligand for the Vn 307-320 domain. The fact that Vn$_{307\text{-}320Mo}$ (Fig. 7) and Vn$_{RGD}$ (Danilov and Juliano, 1989) are both able to substitute for the whole Vn molecule in the axonal growth phenomenon is consistent with the hypothesis that PrP^C and integrins act through the same signal transduction pathway. Notably, the data showing that Vn$_{RGD}$ is able to inhibit axonal growth in wild-type neurons highlights the importance of the integrins in this process.

In spite of the important functions for PrP^C described over the past few years (Chiarini et al., 2002; Lopes et al., 2005; Mouillet-Richard et al., 2000; Rambold et al., 2006; Steele et al., 2006), PrP^C-null mice have only minor defects (Bueler et al., 1992). One explanation for this near-normal phenotype is that PrP^C ablation may be compensated by proteins with redundant functions (Bueler et al., 1992). This seems to be the case here, because the whole Vn molecule induced DRG axonal growth in both wild-type and PrP^C-null neurons. On the other hand, PrP^C-null (both ZrchI and Npu) DRG axonal growth is more sensitive to RGD than the wild-type, indicating that the cellular signaling involved in this phenomenon is more dependent upon integrins in neurons from the knockout animals. Additionally, we observed 30% more activated αvβ3 in DRG from PrP^C-null mice than in their wild-type counterparts. This increase in activated integrins may represent a compensatory mechanism developed by the PrP^C-null animals, where the use of proteins already involved in this specific phenotype can prevent malformation of the nervous system.

Numerous examples of compensatory mechanisms have been reported (Kitami and Nadeau, 2002; Schwarz et al., 2002) and promiscuous cell signaling transduction pathways are targets for molecular redundancy (Xian et al., 2001). Indeed, PrP^C-null mice have been reported to have hyper-activation of extracellular signal-related kinase (ERK) (Chiarini et al., 2002; Lopes et al., 2005; Brown et al., 2002). PrP^C (Zanata et al., 2002b) and integrins (Roberts et al., 2003) are upstream MAPK effectors, which means that at least in this situation, an integrin could substitute for PrP^C signaling.

GPI-anchored proteins, such as PrP^C, can perform signaling roles, integrating the ECM with the cytoskeleton. For example the GPI-anchored raft-associated protein urokinase type plasminogen activator receptor (uPAR) performs complex signaling involved in cell adhesion, proliferation and migration in response to several ligands including Vn (Blasi and Carmeliet, 2002). To modulate internal cell signaling, GPI-anchored proteins must interact with transmembrane adaptors, such as integrins, G-protein-coupled receptors and caveolins (Blasi and Carmeliet, 2002). Despite the involvement of uPAR in cell signaling and diverse biological functions, uPAR-null mice have an apparently normal phenotype (Bugge et al., 1995). Thus, a GPI-anchored protein can be associated with critical regulatory cell tasks and the lack of a severe phenotype in knockout mice cannot demonstrate that the protein is not normally involved in important phenotypes.

In summary, the characterization of PrP^C as a ligand for Vn and its involvement in axonal growth allowed us to demonstrate the relevance of PrP^C in the development of the peripheral nervous system (PNS). Additionally, compensatory mechanisms occurring during embryogenesis are turned on when PrP^C is ablated. Thus, at least for this event, our findings indicate that redundancy for PrP^C interactions resides within the integrin pathway. The importance of PrP^C in the PNS has been increasingly recognized because PNS is a target for PrP^C conversion to PrP^{Sc}, and thus is critically involved in the prion neuroinvasion (Glatzel et al., 2004). Providing further support for PNS involvement in prion neuroinvasion, are the observations that PrP^C is retrogradely transported in peripheral nerves (Moya et al., 2004) and that prion accumulation occurs in DRG and in autonomic ganglia isolated from patients with Creutzfeldt-Jakob and Gerstmann-Sträussler-Scheinker (Haik et al., 2003; Ishida et al., 2005; Lee et al., 2005). The present findings together with these previous observations indicate that the physiological functions of PrP^C in peripheral nerves warrant further investigation.

Materials and Methods

Proteins

Vn and Fn were purified from human plasma (Engvall and Ruoslahti, 1977; Yatohgo et al., 1988) and mouse His$_6$-PrP^C was cloned (Zahn et al., 1997) and expressed (Zanata et al., 2002b). Type IV collagen and albumin are from Sigma. Four PrP^C deletion mutants were constructed using wild-type cDNA by sequential PCR amplification (Ausubel et al., 1993); cloned into pRSET A vector (Invitrogen) and expressed and purified as the wild-type His$_6$-PrP^C. Mutant His$_6$-PrP^C molecules are soluble, sensitive to proteinase K and posses nearly the same α-helix and β-sheet content as the wild-type protein. The following internal primers were used for sequential PCR amplification: Δ51-900R-TACCCCCTCCTGGGTAACGGTTG-CCTCC; F-GAGGGATCCAAAAAGCGGCCAAAG; Δ105-112R-CCAGCTGC-CGCAGCCCCTGGTTGGCTGG; F-CCCAGCAAACCAGGGGCTGCGGCAGC-TGG; Δ113-119R-CCCCATTACTGCCACATGCTTGAGGTTG; F-AAGCATGT-GGCAGTAGTGGGGGGCCTT; Δ120-125R-CAGCATGTAGCCTGCCCCAGC-TGCCGC; F-GCAGCTGGGGCAGGCTACATGCGGGAGC; Δ105-128F-GGAA-CAAGCCCAGCAAACCACTGGGGAGCGCCATGACGG; R-GTCCATGGCGC-TCCCCAGTGGTTTGCTGGGCTTTGTTCC. The following external primers were used for all mutants: F-AGAGAATTCTCAGCTGGATCTTCTCCCGTC; R-GAG-GGATCCAAAAAGCGGCCAAAG.

Peptides

Twenty peptides covering the whole mouse PrP^C (23-231) (Zanata et al., 2002b) were used. STI1 peptide (230-ELGNDAYKKKDFDKAL-245) (Zanata et al., 2002b), laminin γ-1 peptide (1575-RNIAEIIKDI-1584) (Graner et al., 2000a) and six Vn peptides: Vn$_{RGD}$ KPQVTRGDVFTMPE; Vn$_{161\text{-}174}$ AEEELCSGKPFDAF; Vn$_{262\text{-}275}$ AHSYSGRERVYFFK; Vn$_{289\text{-}302}$ SQEECEGSSLSAVF; Vn$_{309\text{-}322Hu}$ QRDSWEDIFELLFW and Vn$_{307\text{-}320Mo}$ QRDSWENIFELLFW were synthesized by Neosystem (Strasbourg, France). The subscript numbers indicate amino acid position in the Vn molecule; the first five peptides follow the human (Hu) Vn sequence and the last one follows the mouse (Mo) Vn sequence.

Antibodies

Anti-PrP^C used for western blotting, immunohistochemistry and immunofluorescence reactions is a polyclonal antibody obtained by His$_6$-PrP^C immunization in PrP^C-null mice. Rabbit polyclonal antibodies obtained by His$_6$-PrP^C (Bethyl) or PrP^C peptide 106-126 (Neosystem) immunization were used in DRG axon growth assays (Chiarini et al., 2002; Zanata et al., 2002b).

The WOW-1 antibody, kindly provided by Prof. Sanford Shattil (University of California), recognizes the active form of αvβ3; the heavy chain hypervariable region of an antibody against activated αIIbβ3 was replaced with a single αv integrin-binding domain (from an adenovirus RGD-rich protein involved in its internalization mediated by αv) (Felding-Habermann et al., 2001; Pampori et al., 1999). The AP5 antibody (GTI Diagnostics) is an anti-LIBS antibody that recognizes the β3 N-terminus and is regulated by cation binding at a site distinct from the LIBS (Honda et al., 1995). At normal extracellular Ca^{2+} levels, AP5 binds

to β3 only when the integrin is in the 'activated' conformation (Faccio et al., 2002). Anti-GFP was from Becton Dickinson and anti-Vn was obtained by rabbit immunization with purified Vn.

Overlay assay

The indicated amounts of Ln, Fn, Vn, type IV collagen and BSA were adsorbed onto nitrocellulose membranes. Blocking was performed in 5% milk in TBST (TBS 0.05% pH 7.4 Tween-20) for 2 hours at room temperature and membranes were then washed. His_6-PrP^C (7 μg) was labeled with 0.5 mCi $Na^{125}I$ (Amersham Biosciences) using one iodobead (Pierce). The labeled protein was incubated with the membrane for 16 hours at 4°C. After washing, an X-ray film (Hyperfilm, Amersham Biosciences) was exposed to the membrane.

3 μg His_6-PrP^C or PrP^C peptides 43-62 or 103-122 was adsorbed onto nitrocellulose membranes. After blocking, $Vn_{307\text{-}320Mo}$ was labeled with biotin using an EZ-Link Sulfo-NHS-LC-Biotinylation Kit (Pierce) and incubated with the membrane for 16 hours at 4°C, followed by Streptavidin-HRP (Sigma) for 1 hour at room temperature.

Binding assays

Binding experiments were conducted as previously described (Graner et al., 2000a; Martins et al., 1997). Briefly, His_6-PrP^C or His_6-PrP^C deletion mutants (2 μg) were adsorbed in polystyrene wells and blocked with 2% BSA. Wells were incubated for 3 hours at 37°C with $Na^{125}I$-labeled Vn or $Vn_{307\text{-}320Mo}$ coupled to BSA. The wells were washed, and radioactivity was measured in a gamma counter (Mini gamma counter, LKB-Wallac). Data were analyzed using the Scatchard Method (Scatchard, 1949).

Competition assays

Unlabeled PrP^C peptides (32 μM) were pre-incubated with 38 nM of ^{125}I-Vn for 2 hours at room temperature. Peptides and ^{125}I-Vn were added to the His_6-PrP^C coated wells and incubated for 3 hours at 37°C. The wells were washed and the radioactivity was measured. Vn, STI1, Ln whole proteins or STI1 and Ln peptides were pre-incubated with coated His_6-PrP^C for 2 hours at room temperature followed by 3 hours at 37°C with ^{125}I-Vn. After washing, the radioactivity was measured.

Cell transfection and pull-down assay

HEK293 cells were transfected with pEGFP-C1 (Clontech) or pEGFP-STI1 (Zanata et al., 2002b) by calcium phosphate co-precipitation as previously described (Puchel et al., 1995). After 48 hours in culture, transfected cells were lysed in NP40 (0.5% in PBS). Cell extracts were pre-cleared by treatment with 30 μl of inactive CNBr-Sepharose (reactive groups previously blocked) for 1 hour at 4°C.

Vn was covalently coupled to CNBr-Sepharose 4B (Amersham) according to the manufacturer's instructions, and 30 μl Vn-CNBr-Sepharose was incubated in pre-cleared cell extracts for 16 hours at 4°C. After washing with 0.5% NP-40 in PBS, bound proteins were eluted with Laemmli buffer and analyzed by western blotting using mouse anti-PrP^C (1:1000) or anti-GFP (1:3000) followed by anti-mouse HRP.

Alexa Fluor 568 Vn labeling and co-localization assay

Vn labeling was performed using an Alexa Fluor 568 labeling kit (Molecular Probes). SN-56 cells, a mouse cholinergic septal neuronal cell line (Blusztajn et al., 1992; Hammond et al., 1990), were transfected with GFP-PrP^C using lipofectamine (Invitrogen) as described previously (Lee et al., 2001). Transfected and differentiated (1 mM cAMP for 1 day) SN-56 cells, were treated with 4 μg Alexa 568-Vn for 1 hour at 4°C. After several washes with PBS, images of live cells were acquired using a Bio-Rad Radiance 2100 laser-scanning confocal system coupled to a Nikon microscope (TE2000-U). Dissociated DRG cells were incubated with 4 μg labelled Vn for 1 hour at 4°C, fixed, submitted to immunofluorescence using mouse anti-PrP^C followed by anti-mouse Alexa Fluor 488, and images were acquired as for SN-56 cells.

Animals

The 'Principles of laboratory animal care' (NIH publication 85-23, 1996) were strictly followed in all experiments. ZrchI $Prnp^{0/0}$ were provided by Dr Charles Weissmann (Scripps Florida, FL) (Bueler et al., 1992). ZrchI $Prnp^{+/+}$ mice were generated by crossing F1 descendants from 129/SV and C57BL/6J matings. Npu $Prnp^{-/-}$ (Manson et al., 1994) were provided by Bruce Chesebro and Richard Race (Rocky Mountain Laboratories, National Institute of Allergy and Infectious Diseases, MT). These animals were backcrossed to C57BL/10 mice for at least eight generations. Heterozygous animals were mated and homozygous F1 descendants from the same litter were crossed to generate Npu $Prnp^{-/-}$ or Npu $Prnp^{+/+}$ embryos. All of the adult animals used to generate Npu $Prnp^{-/-}$ and Npu $Prnp^{+/+}$ embryos were genotyped by PCR (Manson et al., 1994).

DRG explants

DRG from E12.5 mice (Bueler et al., 1992) were dissected and cultured in poly-L-lysine coated glass coverslip in neurobasal medium (Invitrogen) with 2 mM glutamine, 100 IU penicillin, 100 μg/ml streptomicyn, B-27 (Invitrogen) and 50 ng/ml nerve growth factor (Sigma). In Fig. 7b,d, DRGs were plated in Vn_{RGD}-BSA adsorbed coverslips. Treatments were performed immediately after plating and ganglia were cultured for 24 (Fig. 6i,j, Fig. 7a-c) or 36 hours (Fig. 6a-h), fixed in 4% paraformaldehyde/0.12 M sucrose and stained with haematoxylin. The neurite length was measured as the distance from the edge of the DRG to the tip of the three longest neurites, and the mean value was used as the neurite length for each DRG (Zanata et al., 2002a). At least 12 ganglia from three independent experiments were considered for each individual data point. Cultures were dissociated by enzymatic digestion of the dissected ganglia for 30 minutes with 1% trypsin in neurobasal medium. After mechanical dissociation, 5×10^4 cells per 13 mm^2 well were plated in the presence of Vn for 6 hours. Cells were fixed and stained as described above and the percentage of cells presenting a neurite longer than one cell body was calculated.

Immunohistochemistry

DRG explants grown in the presence of Vn were fixed and incubated for 4 hours at 4°C with a mouse polyclonal antibody anti-PrP^C, 1:250 (Chiarini et al., 2002) followed by Alexa Fluor 568 anti-mouse IgG (Molecular Probes, Eugene, OR), for 40 minutes at room temperature. Ganglia were viewed with an Olympus IX70 microscope equipped with epifluorescence.

Formalin-fixed E12.5 mice embryos were embedded in paraffin and sections submitted to immunohistochemistry as previously described (Lopes et al., 2005) with mouse polyclonal anti-PrP^C antibody (1:1000) (Chiarini et al., 2002) or with rabbit polyclonal anti-Vn antibody (1:250).

Confocal immunofluorescence

E12.5 mouse embryos were immediately frozen and 3-μm-thick cryostat sections submitted to immunofluorescence as previously described (Lopes et al., 2005) with a mouse polyclonal anti-PrP^C antibody (1:250) (Chiarini et al., 2002) and rabbit anti-Vn serum (1:100).

αvβ3 activity assays

Dissociated DRG cells were plated on poly-L-lysine-coated coverslips and incubated for 24 hours, fixed, and blocked as described above. Immunofluorescence reaction with WOW-1 antibody (1:4) (Pampori et al., 1999) was undertaken for 16 hours at room temperature followed by Alexa Fluor 568 anti-mouse IgG (1:3000) (Molecular Probes). Immunofluorescence with AP5 antibody (50 μg/ml) was performed in PBS with 3 mM Ca^{2+} for 16 hours at room temperature followed by Alexa Fluor 568 anti-mouse IgG (1:3000). Images were acquired with an Olympus IX70 microscope equipped with epifluorescence. To acquire the images, the digital camera (Olympus DP70) exposure was set so that no fluorescence could be observed in cells incubated with only secondary antibody. At least five fields of each coverslip were imaged and the fluorescence of each cell was measured with the Image-Pro Plus 4.1 (Media Cybernetics). At least 100 cells per coverslip were considered.

Statistical analysis

The mean values of at least three independent datasets are shown in the figures; the error bars represent s.d. Fit to a normal distribution was evaluated with the Kolmogorov-Smirnov test. The homogeneity of variances was assessed using Levene's test. The comparison of means for two independent samples was performed using Student's *t*-test or Mann-Whitney's test. When comparing more than two groups, an ANOVA or Kruskal Wallis test was used and a Tukey-HSD test was used for multiple comparisons.

This work was supported by FAPESP (Fundação de Amparo a Pesquisa do Estado de São Paulo) (99/07124-8 and 03-13189-2) and V.R.M. is supported by the Howard Hughes Medical Institute. G.N.M.H., M.H.L. and T.G.S. are fellows from FAPESP. We are grateful to Ricardo Brentani for helpful discussions. We acknowledge Sanford Shattil for providing WOW antibody and Bruce Chesebro, Richard Race and Charles Weissmann for providing the PrP^C-null mice. We dedicate this work to the memory of Saul Jacchieri, an extraordinarily bright example of a life dedicated to science.

References

Ausubel, F. M., Brent, R., Kingston, R. E., Moore, D. D., Seidman, J. D., Smith, J. A. and Struhl, K. (1993). Constructing recombinant DNA molecules by the polymerase chain reaction. In *Current Protocols in Molecular Biology* (1st edn), p. 3.17.1. New York: Wiley Interscience.

Blasi, F. and Carmeliet, P. (2002). uPAR: a versatile signalling orchestrator. *Nat. Rev. Mol. Cell Biol.* **3**, 932-943.

Blusztajn, J. K., Venturini, A., Jackson, D. A., Lee, H. J. and Wainer, B. H. (1992). Acetylcholine synthesis and release is enhanced by dibutyryl cyclic AMP in a neuronal cell line derived from mouse septum. *J. Neurosci.* **12**, 793-799.

Brentani, R. R. (1988). Biological implications of complementary hydropathy of amino acids. *J. Theor. Biol.* **135**, 495-499.

Brown, D. R. and Besinger, A. (1998). Prion protein expression and superoxide dismutase activity. *Biochem. J.* **334**, 423-429.

Brown, D. R., Qin, K., Herms, J. W., Madlung, A., Manson, J., Strome, R., Fraser, P. E., Kruck, T., von Bohlen, A., Schulz-Schaeffer, W. et al. (1997). The cellular prion protein binds copper in vivo. *Nature* **390**, 684-687.

Brown, D. R., Nicholas, R. S. and Canevari, L. (2002). Lack of prion protein expression results in a neuronal phenotype sensitive to stress. *J. Neurosci. Res.* **67**, 211-224.

Bueler, H., Fischer, M., Lang, Y., Bluethmann, H., Lipp, H. P., DeArmond, S. J., Prusiner, S. B., Aguet, M. and Weissmann, C. (1992). Normal development and behaviour of mice lacking the neuronal cell-surface PrP protein. *Nature* **356**, 577-582.

Bugge, T. H., Suh, T. T., Flick, M. J., Daugherty, C. C., Romer, J., Solberg, H., Ellis, V., Dano, K. and Degen, J. L. (1995). The receptor for urokinase-type plasminogen activator is not essential for mouse development or fertility. *J. Biol. Chem.* **270**, 16886-16894.

Chen, S., Mange, A., Dong, L., Lehmann, S. and Schachner, M. (2003). Prion protein as trans-interacting partner for neurons is involved in neurite outgrowth and neuronal survival. *Mol. Cell. Neurosci.* **22**, 227-233.

Chen, Z. L., Indyk, J. A. and Strickland, S. (2003). The hippocampal laminin matrix is dynamic and critical for neuronal survival. *Mol. Biol. Cell* **14**, 2665-2676.

Chiarini, L. B., Freitas, A. R., Zanata, S. M., Brentani, R. R., Martins, V. R. and Linden, R. (2002). Cellular prion protein transduces neuroprotective signals. *EMBO J.* **21**, 3317-3326.

Coitinho, A. S., Freitas, A. R., Lopes, M. H., Hajj, G. N., Roesler, R., Walz, R., Rossato, J. I., Cammarota, M., Izquierdo, I., Martins, V. R. et al. (2006). The interaction between prion protein and laminin modulates memory consolidation. *Eur. J. Neurosci.* **24**, 3255-3264.

Cordeiro, Y., Kraineva, J., Ravindra, R., Lima, L. M., Gomes, M. P., Foguel, D., Winter, R. and Silva, J. L. (2004a). Hydration and packing effects on prion folding and beta-sheet conversion. High pressure spectroscopy and pressure perturbation calorimetry studies. *J. Biol. Chem.* **279**, 32354-32359.

Cordeiro, Y., Lima, L. M., Gomes, M. P., Foguel, D. and Silva, J. L. (2004b). Modulation of prion protein oligomerization, aggregation, and beta-sheet conversion by 4,4′-dianilino-1,1′-binaphthyl-5,5′-sulfonate (bis-ANS). *J. Biol. Chem.* **279**, 5346-5352.

Danilov, Y. N. and Juliano, R. L. (1989). (Arg-Gly-Asp)n-albumin conjugates as a model substratum for integrin-mediated cell adhesion. *Exp. Cell Res.* **182**, 186-196.

Easley, C. A., Faison, M. O., Kirsch, T. L., Lee, J. A., Seward, M. E. and Tombes, R. M. (2006). Laminin activates CaMK-II to stabilize nascent embryonic axons. *Brain Res.* **1092**, 59-68.

Engvall, E. and Ruoslahti, E. (1977). Binding of soluble form of fibroblast surface protein, fibronectin, to collagen. *Int. J. Cancer* **20**, 1-5.

Ettaiche, M., Pichot, R., Vincent, J. P. and Chabry, J. (2000). In vivo cytotoxicity of the prion protein fragment 106-126. *J. Biol. Chem.* **275**, 36487-36490.

Faccio, R., Grano, M., Colucci, S., Villa, A., Giannelli, G., Quaranta, V. and Zallone, A. (2002). Localization and possible role of two different alpha v beta 3 integrin conformations in resting and resorbing osteoclasts. *J. Cell Sci.* **115**, 2919-2929.

Felding-Habermann, B. and Cheresh, D. A. (1993). Vitronectin and its receptors. *Curr. Opin. Cell Biol.* **5**, 864-868.

Felding-Habermann, B., O'Toole, T. E., Smith, J. W., Fransvea, E., Ruggeri, Z. M., Ginsberg, M. H., Hughes, P. E., Pampori, N., Shattil, S. J., Saven, A. et al. (2001). Integrin activation controls metastasis in human breast cancer. *Proc. Natl. Acad. Sci. USA* **98**, 1853-1858.

Francois, P. P., Preissner, K. T., Herrmann, M., Haugland, R. P., Vaudaux, P., Lew, D. P. and Krause, K. H. (1999). Vitronectin interaction with glycosaminoglycans. Kinetics, structural determinants, and role in binding to endothelial cells. *J. Biol. Chem.* **274**, 37611-37619.

Gabriel, J. M., Oesch, B., Kretzschmar, H., Scott, M. and Prusiner, S. B. (1992). Molecular cloning of a candidate chicken prion protein. *Proc. Natl. Acad. Sci. USA* **89**, 9097-9101.

Gartner, T. K., Loudon, R. and Taylor, D. B. (1991). The peptides APLHK, EHIPA and GAPL are hydropathically equivalent peptide mimics of a fibrinogen binding domain of glycoprotein IIb/IIIa. *Biochem. Biophys. Res. Commun.* **180**, 1446-1452.

Gauczynski, S., Peyrin, J. M., Haik, S., Leucht, C., Hundt, C., Rieger, R., Krasemann, S., Deslys, J. P., Dormont, D., Lasmezas, C. I. et al. (2001). The 37-kDa/67-kDa laminin receptor acts as the cell-surface receptor for the cellular prion protein. *EMBO J.* **20**, 5863-5875.

Glatzel, M., Giger, O., Braun, N. and Aguzzi, A. (2004). The peripheral nervous system and the pathogenesis of prion diseases. *Curr. Mol. Med.* **4**, 355-359.

Gonzalez-Iglesias, R., Pajares, M. A., Ocal, C., Espinosa, J. C., Oesch, B. and Gasset, M. (2002). Prion protein interaction with glycosaminoglycan occurs with the formation of oligomeric complexes stabilized by Cu(II) bridges. *J. Mol. Biol.* **319**, 527-540.

Graner, E., Mercadante, A. F., Zanata, S. M., Forlenza, O. V., Cabral, A. L., Veiga, S. S., Juliano, M. A., Roesler, R., Walz, R., Minetti, A. et al. (2000a). Cellular prion protein binds laminin and mediates neuritogenesis. *Brain Res. Mol. Brain Res.* **76**, 85-92.

Graner, E., Mercadante, A. F., Zanata, S. M., Martins, V. R., Jay, D. G. and Brentani, R. R. (2000b). Laminin-induced PC-12 cell differentiation is inhibited following laser inactivation of cellular prion protein. *FEBS Lett.* **482**, 257-260.

Haik, S., Faucheux, B. A., Sazdovitch, V., Privat, N., Kemeny, J. L., Perret-Liaudet, A. and Hauw, J. J. (2003). The sympathetic nervous system is involved in variant Creutzfeldt-Jakob disease. *Nat. Med.* **9**, 1121-1123.

Hammond, D. N., Lee, H. J., Tonsgard, J. H. and Wainer, B. H. (1990). Development and characterization of clonal cell lines derived from septal cholinergic neurons. *Brain Res.* **512**, 190-200.

Heal, J. R., Roberts, G. W., Raynes, J. G., Bhakoo, A. and Miller, A. D. (2002). Specific interactions between sense and complementary peptides: the basis for the proteomic code. *Chembiochem.* **3**, 136-151.

Honda, S., Tomiyama, Y., Pelletier, A. J., Annis, D., Honda, Y., Orchekowski, R., Ruggeri, Z. and Kunicki, T. J. (1995). Topography of ligand-induced binding sites, including a novel cation-sensitive epitope (AP5) at the amino terminus, of the human integrin beta 3 subunit. *J. Biol. Chem.* **270**, 11947-11954.

Hundt, C., Peyrin, J. M., Haik, S., Gauczynski, S., Leucht, C., Rieger, R., Riley, M. L., Deslys, J. P., Dormont, D., Lasmezas, C. I. et al. (2001). Identification of interaction domains of the prion protein with its 37-kDa/67-kDa laminin receptor. *EMBO J.* **20**, 5876-5886.

Hynes, R. O. (2002). Integrins: bidirectional, allosteric signaling machines. *Cell* **110**, 673-687.

Isahara, K. and Yamamoto, M. (1995). The interaction of vascular endothelial cells and dorsal root ganglion neurites is mediated by vitronectin and heparan sulfate proteoglycans. *Brain Res. Dev. Brain Res.* **84**, 164-178.

Ishida, C., Okino, S., Kitamoto, T. and Yamada, M. (2005). Involvement of the peripheral nervous system in human prion diseases including dural graft associated Creutzfeldt-Jakob disease. *J. Neurol. Neurosurg. Psychiatr.* **76**, 325-329.

Jimenez-Huete, A., Lievens, P. M., Vidal, R., Piccardo, P., Ghetti, B., Tagliavini, F., Frangione, B. and Prelli, F. (1998). Endogenous proteolytic cleavage of normal and disease-associated isoforms of the human prion protein in neural and non-neural tissues. *Am. J. Pathol.* **153**, 1561-1572.

Kitami, T. and Nadeau, J. H. (2002). Biochemical networking contributes more to genetic buffering in human and mouse metabolic pathways than does gene duplication. *Nat. Genet.* **32**, 191-194.

Lee, C. C., Kuo, L. T., Wang, C. H., Scaravilli, F. and An, S. F. (2005). Accumulation of prion protein in the peripheral nervous system in human prion diseases. *J. Neuropathol. Exp. Neurol.* **64**, 716-721.

Lee, K. S., Magalhaes, A. C., Zanata, S. M., Brentani, R. R., Martins, V. R. and Prado, M. A. (2001). Internalization of mammalian fluorescent cellular prion protein and N-terminal deletion mutants in living cells. *J. Neurochem.* **79**, 79-87.

Lee, K. S., Linden, R., Prado, M. A., Brentani, R. R. and Martins, V. R. (2003). Towards cellular receptors for prions. *Rev. Med. Virol.* **13**, 399-408.

Lopes, M. H., Hajj, G. N., Muras, A. G., Mancini, G. L., Castro, R. M., Ribeiro, K. C., Brentani, R. R., Linden, R. and Martins, V. R. (2005). Interaction of cellular prion and stress-inducible protein 1 promotes neuritogenesis and neuroprotection by distinct signaling pathways. *J. Neurosci.* **25**, 11330-11339.

Manson, J. C., Clarke, A. R., Hooper, M. L., Aitchison, L., McConnell, I. and Hope, J. (1994). 129/Ola mice carrying a null mutation in PrP that abolishes mRNA production are developmentally normal. *Mol. Neurobiol.* **8**, 121-127.

Martinez-Morales, J. R., Marti, E., Frade, J. M. and Rodriguez-Tebar, A. (1995). Developmentally regulated vitronectin influences cell differentiation, neuron survival and process outgrowth in the developing chicken retina. *Neuroscience* **68**, 245-253.

Martinez-Morales, J. R., Barbas, J. A., Marti, E., Bovolenta, P., Edgar, D. and Rodriguez-Tebar, A. (1997). Vitronectin is expressed in the ventral region of the neural tube and promotes the differentiation of motor neurons. *Development* **124**, 5139-5147.

Martins, V. R. and Brentani, R. R. (2002). The biology of the cellular prion protein. *Neurochem. Int.* **41**, 353-355.

Martins, V. R., Graner, E., Garcia-Abreu, J., de Souza, S. J., Mercadante, A. F., Veiga, S. S., Zanata, S. M., Neto, V. M. and Brentani, R. R. (1997). Complementary hydropathy identifies a cellular prion protein receptor. *Nat. Med.* **3**, 1376-1382.

Mastrianni, J. A. and Roos, R. P. (2000). The prion diseases. *Semin. Neurol.* **20**, 337-352.

Miele, G., Alejo Blanco, A. R., Baybutt, H., Horvat, S., Manson, J. and Clinton, M. (2003). Embryonic activation and developmental expression of the murine prion protein gene. *Gene Expr.* **11**, 1-12.

Monier-Gavelle, F. and Duband, J. L. (1997). Cross talk between adhesion molecules: control of N-cadherin activity by intracellular signals elicited by beta1 and beta3 integrins in migrating neural crest cells. *J. Cell Biol.* **137**, 1663-1681.

Mouillet-Richard, S., Ermonval, M., Chebassier, C., Laplanche, J. L., Lehmann, S., Launay, J. M. and Kellermann, O. (2000). Signal transduction through prion protein. *Science* **289**, 1925-1928.

Moya, K. L., Hassig, R., Creminon, C., Laffont, I. and Di Giamberardino, L. (2004). Enhanced detection and retrograde axonal transport of PrPc in peripheral nerve. *J. Neurochem.* **88**, 155-160.

Oesch, B., Westaway, D., Walchli, M., McKinley, M. P., Kent, S. B., Aebersold, R., Barry, R. A., Tempst, P., Teplow, D. B., Hood, L. E. et al. (1985). A cellular gene encodes scrapie PrP 27-30 protein. *Cell* **40**, 735-746.

Pampori, N., Hato, T., Stupack, D. G., Aidoudi, S., Cheresh, D. A., Nemerow, G. R. and Shattil, S. J. (1999). Mechanisms and consequences of affinity modulation of integrin alpha(V)beta(3) detected with a novel patch-engineered monovalent ligand. *J. Biol. Chem.* **274**, 21609-21616.

Pan, T., Wong, B. S., Liu, T., Li, R., Petersen, R. B. and Sy, M. S. (2002). Cell-surface prion protein interacts with glycosaminoglycans. *Biochem. J.* **368**, 81-90.

Pierschbacher, M. D. and Ruoslahti, E. (1984). Cell attachment activity of fibronectin can be duplicated by small synthetic fragments of the molecule. *Nature* **309**, 30-33.

Pierschbacher, M. D. and Ruoslahti, E. (1987). Influence of stereochemistry of the sequence Arg-Gly-Asp-Xaa on binding specificity in cell adhesion. *J. Biol. Chem.* **262**, 17294-17298.

Pons, S. and Marti, E. (2000). Sonic hedgehog synergizes with the extracellular matrix protein vitronectin to induce spinal motor neuron differentiation. *Development* **127**, 333-342.

Pons, S., Trejo, J. L., Martinez-Morales, J. R. and Marti, E. (2001). Vitronectin regulates Sonic hedgehog activity during cerebellum development through CREB phosphorylation. *Development* **128**, 1481-1492.

Preissner, K. T. (1991). Structure and biological role of vitronectin. *Annu. Rev. Cell Biol.* **7**, 275-310.

Puschel, A. W., Adams R. H. and Betz, H. (1995). Murine semaphoring D/collapsing is a member of a diverse gene family and creates domains inhibitory for axonal growth. *Neuron* **14**, 941-948.

Rambold, A. S., Miesbauer, M., Rapaport, D., Bartke, T., Baier, M., Winklhofer, K. F. and Tatzelt, J. (2006). Association of Bcl-2 with misfolded prion protein is linked to the toxic potential of cytosolic PrP. *Mol. Biol. Cell* **17**, 3356-3368.

Riek, R., Hornemann, S., Wider, G., Billeter, M., Glockshuber, R. and Wuthrich, K. (1996). NMR structure of the mouse prion protein domain PrP(121-321). *Nature* **382**, 180-182.

Roberts, M. S., Woods, A. J., Shaw, P. E. and Norman, J. C. (2003). ERK1 associates with alpha(v)beta 3 integrin and regulates cell spreading on vitronectin. *J. Biol. Chem.* **278**, 1975-1985.

Ruoslahti, E. and Pierschbacher, M. D. (1987). New perspectives in cell adhesion: RGD and integrins. *Science* **238**, 491-497.

Sales, N., Hassig, R., Rodolfo, K., Di Giamberardino, L., Traiffort, E., Ruat, M., Fretier, P. and Moya, K. L. (2002). Developmental expression of the cellular prion protein in elongating axons. *Eur. J. Neurosci.* **15**, 1163-1177.

Santuccione, A., Sytnyk, V., Leshchyns'ka, I. and Schachner, M. (2005). Prion protein recruits its neuronal receptor NCAM to lipid rafts to activate p59fyn and to enhance neurite outgrowth. *J. Cell Biol.* **169**, 341-354.

Scatchard, G. (1949). The attractions of proteins for small molecules and ions. *Ann. N. Y. Acad. Sci.* **51**, 666-672.

Schmitt-Ulms, G., Legname, G., Baldwin, M. A., Ball, H. L., Bradon, N., Bosque, P. J., Crossin, K. L., Edelman, G. M., DeArmond, S. J., Cohen, F. E. et al. (2001). Binding of neural cell adhesion molecules (N-CAMs) to the cellular prion protein. *J. Mol. Biol.* **314**, 1209-1225.

Schvartz, I., Seger, D. and Shaltiel, S. (1999). Vitronectin. *Int. J. Biochem. Cell Biol.* **31**, 539-544.

Schwarz, D. G., Griffin, C. T., Schneider, E. A., Yee, D. and Magnuson, T. (2002). Genetic analysis of sorting nexins 1 and 2 reveals a redundant and essential function in mice. *Mol. Biol. Cell* **13**, 3588-3600.

Seiffert, D., Iruela-Arispe, M. L., Sage, E. H. and Loskutoff, D. J. (1995). Distribution of vitronectin mRNA during murine development. *Dev. Dyn.* **203**, 71-79.

Steele, A. D., Emsley, J. G., Ozdinler, P. H., Lindquist, S. and Macklis, J. D. (2006). Prion protein (PrPc) positively regulates neural precursor proliferation during developmental and adult mammalian neurogenesis. *Proc. Natl. Acad. Sci. USA* **103**, 3416-3421.

Takagi, J., Petre, B. M., Walz, T. and Springer, T. A. (2002). Global conformational rearrangements in integrin extracellular domains in outside-in and inside-out signaling. *Cell* **110**, 599-511.

Tom, V. J., Doller, C. M., Malouf, A. T. and Silver, J. (2004). Astrocyte-associated fibronectin is critical for axonal regeneration in adult white matter. *J. Neurosci.* **24**, 9282-9290.

Tsai, C. J., Lin, S. L., Wolfson, H. J. and Nussinov, R. (1997). Studies of protein-protein interfaces: a statistical analysis of the hydrophobic effect. *Protein Sci.* **6**, 53-64.

Turney, S. G. and Bridgman, P. C. (2005). Laminin stimulates and guides axonal outgrowth via growth cone myosin II activity. *Nat. Neurosci.* **8**, 717-719.

Xian, C. J., Li, L., Deng, Y. S., Zhao, S. P. and Zhou, X. F. (2001). Lack of effects of transforming growth factor-alpha gene knockout on peripheral nerve regeneration may result from compensatory mechanisms. *Exp. Neurol.* **172**, 182-188.

Xu, D., Baburaj, K., Peterson, C. B. and Xu, Y. (2001). Model for the three-dimensional structure of vitronectin: predictions for the multi-domain protein from threading and docking. *Proteins* **44**, 312-320.

Xu, Y. and Xu, D. (2000). Protein threading using PROSPECT: design and evaluation. *Proteins* **40**, 343-354.

Yatohgo, T., Izumi, M., Kashiwagi, H. and Hayashi, M. (1988). Novel purification of vitronectin from human plasma by heparin affinity chromatography. *Cell Struct. Funct.* **13**, 281-292.

Zahn, R., von Schroetter, C. and Wuthrich, K. (1997). Human prion proteins expressed in Escherichia coli and purified by high- affinity column refolding. *FEBS Lett.* **417**, 400-404.

Zanata, S. M., Hovatta, I., Rohm, B. and Puschel, A. W. (2002a). Antagonistic effects of Rnd1 and RhoD GTPases regulate receptor activity in Semaphorin 3A-induced cytoskeletal collapse. *J. Neurosci.* **22**, 471-477.

Zanata, S. M., Lopes, M. H., Mercadante, A. F., Hajj, G. N., Chiarini, L. B., Nomizo, R., Freitas, A. R., Cabral, A. L., Lee, K. S., Juliano, M. A. et al. (2002b). Stress-inducible protein 1 is a cell surface ligand for cellular prion that triggers neuroprotection. *EMBO J.* **21**, 3307-3316.